



CHORUS

This is the accepted manuscript made available via CHORUS. The article has been published as:

Raman scattering from biased molecular conduction junctions: The electronic background and its temperature

Michael Galperin and Abraham Nitzan

Phys. Rev. B **84**, 195325 — Published 28 November 2011

DOI: [10.1103/PhysRevB.84.195325](https://doi.org/10.1103/PhysRevB.84.195325)

Raman scattering from biased molecular conduction junctions: The electronic background and its temperature

Michael Galperin^{1,*} and Abraham Nitzan^{2,†}

¹*Department of Chemistry & Biochemistry, University of California at San Diego, La Jolla, CA 92093*

²*School of Chemistry, Tel Aviv University, Tel Aviv, 69978, Israel*

The existence of background in the surface enhanced Raman scattering (SERS) from molecules adsorbed on metal surfaces is known since the early studies this phenomenon, and is usually attributed to transitions between electronic states of the metal substrate. This paper reformulates the theory of this phenomenon in the framework of the non-equilibrium Green function (NEGF) formalism, which makes it possible to extend it to the case of Raman scattering from non-equilibrium (biased and current carrying) molecular junctions. Following recent experiments, we address in particular the Raman scattering measurement of current induced electronic heating. The *Raman temperature*, defined by fitting the ratio between the Stokes and anti-Stokes Raman signals to a Boltzmann factor is compared to another measure of electronic heating obtained by assuming that close to the molecule-metal contact the electronic distribution is dominated by the transmission process. We find that the Raman temperature considerably exceed this upper bound to the metal-electrons heating. In agreement with this observation we show that the Raman temperature reflects the electronic non-equilibrium in the molecular bridge itself. We also show that the Raman temperature concept breaks down at large bias.

PACS numbers: 73.23.-b 78.20.Jq 78.30.-j 78.67.-n

I. INTRODUCTION

Studies of Raman scattering from molecular conduction junctions lie at the juncture of two contemporary fields of research: Molecular electronics, which focuses on the electronic transport properties of molecules connecting between conducting leads, and molecular plasmonics, in particular surface enhanced Raman scattering (SERS), that exploit the behavior of the electromagnetic field near metallic interfaces to enhance and control the optical response of molecules adsorbed at such interfaces. Typical configurations of molecule conduction junctions are similar to structures discussed as “hot spots” in single molecule SERS,^{1–10} that is, structures characterized by strong enhancement of the local electromagnetic field. Indeed, this enhancement was important for getting detectable signals in recent studies of Raman scattering from such junctions^{11–13} Not surprisingly, it was found that the junction conductivity and the Raman scattering signal show correlated behavior,¹¹ indicating that Raman scattering can probe structural changes in the junction that affect its conductivity.¹⁴

Further development of optical methods in the context of molecular conduction junctions is obviously very desirable because interaction with the radiation field can provide new ways of characterization and control of such systems.¹⁷ Many aspects of optical interaction in tunneling junctions have been studied in the past.¹⁸ Among these are observations of light emission from current carrying molecular junctions,^{2,19–21,23–33} affecting junction conduction properties and inducing DC currents by optical signals^{34–40} and using optical pulses to cause conduction switching by affecting structural changes.^{41–51} Relevant to our present discussion are recent demonstrations^{12,13} that it can be used to determine

the effective temperature in biased and current carrying junctions.

This experimental effort has been accompanied by theoretical studies of various phenomena pertaining to what we may call *junction spectroscopy*. Such studies attempt to characterize the correlation between optical response and electrical conduction properties of molecular conduction junctions,^{52–69} and are supplemented by parallel studies of the behavior of optical fields at metallic interfaces pertaining to such junctions.⁷⁰ Recent papers by us and coworkers have addressed current induced light and light induced current phenomena in molecular junctions^{71–73} as well as the possibility to control the latter by properly shaped photon pulses.^{74,75} Another work, presents a general theory of Raman scattering from molecular conduction junctions,^{76,77} and addresses, among other issues, the possibility to use this phenomenon to determine the junction effective temperature. This work provides the starting point for the present discussion.

The present paper addresses recent experimental observations¹² of heating in current carrying tunneling junctions with and without molecular bridges, using Raman scattering as probe. The issue of heating in biased molecular junctions has attracted considerable recent experimental and theoretical attention, motivated by the relevance of this phenomenon to current induced chemical change and to junction stability.^{78,79} This issue was addressed theoretically by several workers,^{80–98} however the experimental observation of such heating^{12,13,99–105} depends on finding a suitable probe. First attempt to estimate junction heating^{100,101} have used the threshold for bond breaking under tension as such a probe. Raman scattering provides a more direct probe that can be in principle applied separately to the different modes by

using the information conveyed by the relative intensities of the corresponding Stokes/anti-Stokes components of scattering signal.^{12,13,76} Indeed, Ward and coworkers¹² were able not only to assign effective temperatures to several molecular vibrations and follow its change as function of bias voltages, but also to address the temperature of the underlying electronic continuum. This observation is, in principle, very significant, since standard treatments of conduction in nanojunctions including molecular junctions usually assume that the metal contacts remain at their original thermal equilibrium. While heating of molecular degrees of freedom was considered by us and others in previous theoretical work, this observation makes it necessary to address contacts electronic heating as well.

Focusing on this issue, several questions should be considered at the outset. First, using Raman scattering as a temperature probe of current induced heating, has the drawback that the incident light can itself heat the system. Indeed, Ward and coworkers¹² find temperature rise associated with junction illumination at zero bias. In the present work we focus on the additional heating associated with electronic conduction in the biased junction. Secondly, bias induced heating is observed also in pure metallic junctions that do not incorporate bridging molecules.¹² Here we focus on molecular junctions characterized by relatively low transmission, where direct charge transfer between metal electrodes can be disregarded.¹⁰⁶ Next, one may question why electronic conduction through the molecular bridge affects heating of electrons in the macroscopic electrodes. The answer is that the molecular current creates a region in the metal, near the metal-molecule contact, where the electronic distribution is out of equilibrium. Because of the fast (10 – 100 fs) relaxation of electrons in metals, this region is very small (a rough estimate based on the Fermi velocity yields ~ 10 nm for its linear size), however Raman scattering, dominated by the molecule-radiation field interaction and affected by the molecule-metal interaction probes exactly this non-equilibrium region. Finally, a general problem in describing heating in non-equilibrium system is the natural desire to describe such heating in terms of a single parameter, an “effective temperature”. As has often been pointed out, this may provide a qualitative indication of heating, but different definitions may yield different numerical values for such “temperature”. These considerations are reflected in the theory forwarded below.

The analysis of electronic heating in Raman scattering experiments is closely related to the general discussion of the continuous background observed in SERS experiment, see, e.g., 107–111 While different origins of this phenomenon were postulated over the years, there seems to be general agreement that this contribution to inelastic light scattering involves excitation of electron-hole pairs in the metal. What makes it difficult to identify a unique mechanism for this phenomenon is that more than one process may be involved. In particular the observed back-

ground may often result from both Raman and fluorescence processes, the latter involving intermediate loss of coherence by dephasing or thermal relaxation. Furthermore, in studies involving metal particles, the fluorescence appears to emanate from plasmon excitations in these particles, suggesting the possibility that plasmons are formed by relaxation of e-h pairs.^{112,113} While our view is somewhat different,¹¹⁴ the relative contribution of Raman and fluorescence processes to the observed inelastic continuum is an important attribute of the process.

Whatever the detailed mechanism(s) of the background scattering/emission is, a corresponding theory will depend on the electronic distribution in the metal substrate, which, for bias-driven junctions should reflect its non-equilibrium character. In the present paper we describe such a theory, using the non-equilibrium Green function (NEGF) technique. Our model is similar to those used earlier for this problem,^{108,109,115,116} however the NEGF methodology makes it possible to generalize these treatments to the non-equilibrium situations that characterize biased molecular junctions. Furthermore, we advance a simple theoretical description of the non-equilibrium electronic distributions at the two metal contacts of the biased junction and use it to estimate the junction heating and the associated electronic Raman spectrum. Our results compare well with the observations of Ref. 12 for reasonable choices of junction parameters, however they also emphasize the difficulties inherent in the use of the effective temperature concept. Furthermore, they place the origin of the observed electronic heating more with the electronic-non equilibrium distribution in the molecular bridge than with that in the metal. A short account focusing on this issue was recently published.¹¹⁷

Our theory of the electronic Raman background in biased molecular junctions is presented in the next section. Irrespective of our later focus on junction heating, this theory makes interesting and testable predictions concerning the bias voltage dependence of this spectrum. In section III we present a simple description of the non-equilibrium electronic distribution at the metal-molecule contact and use it to define a voltage dependent effective temperature. The voltage dependent electronic Raman scattering and the effective temperature associated with its anti-Stokes (AS) component are discussed in Section IV in comparison with the experimental results of Ref. 12. Section V concludes.

II. ELECTRONIC RAMAN SCATTERING IN BIASED MOLECULAR JUNCTIONS

We consider a molecular junction driven by a single mode cw light under current-carrying conditions. The junction consists of a molecule M coupled to two metal contacts L and R , considered to be free electron carriers (Fermi seas) each at its own thermal equilibrium

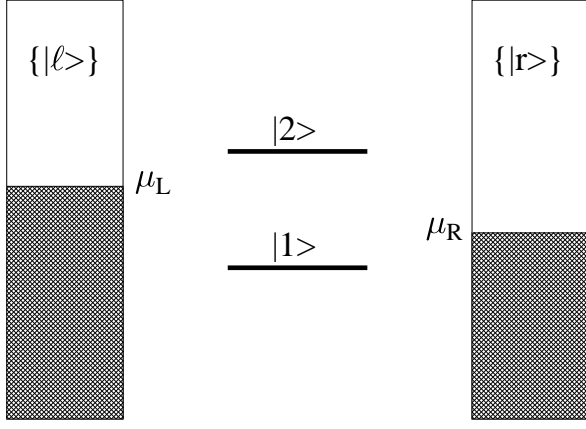


FIG. 1: A two level model for a molecular conduction junction.

characterized by electrochemical potentials μ_L and μ_R , respectively. The molecule is represented by a two-level (HOMO-LUMO) model used in our previous work (Fig. 1).^{70-72,74,76,77,118} We focus only on the contribution to the Raman signal (that is, inelastic light scattering) associated with energy imparted to electronic states in the metals, and therefore omit for simplicity molecular vibrations from our consideration. The electronic inelastic spectrum dresses the Rayleigh scattering signal in the calculation discussed below and it will similarly dress any vibrationally inelastic signal in a calculation that incorporates vibrational motion. The Hamiltonian of the system is

$$\hat{H} = \hat{H}_M + \sum_{K=L,R} (\hat{H}_K + \hat{V}_{KM}) + \hat{H}_{opt} + \hat{V}_{opt,M} \quad (1)$$

where \hat{H}_M is the molecular Hamiltonian, \hat{H}_K ($K = L, R$) are the Hamiltonians of the metal electrodes and \hat{V}_{KM} are the corresponding couplings that represent electron transfer between molecule and electrodes. \hat{H}_{opt} is the Hamiltonian of the radiation field, and $\hat{V}_{opt,M}$ is the molecule-radiation field coupling:

$$\hat{H}_M = \sum_{m=1,2} \varepsilon_m \hat{d}_m^\dagger \hat{d}_m \quad (2)$$

$$\hat{H}_K = \sum_{k \in K} \varepsilon_k \hat{c}_k^\dagger \hat{c}_k \quad (3)$$

$$\hat{V}_{KM} = \sum_{m=1,2} \sum_{k \in K} (V_{km} \hat{c}_k^\dagger \hat{d}_m + \text{H.c.}) \quad (4)$$

$$\hat{H}_{opt} = \sum_{\alpha} \hbar \nu_{\alpha} \hat{a}_{\alpha}^\dagger \hat{a}_{\alpha} \quad (5)$$

$$\hat{V}_{opt,M} = \sum_{\alpha} (U_{\alpha} \hat{a}_{\alpha} \hat{d}_2^\dagger \hat{d}_1 + \text{H.c.}) \quad (6)$$

Here \hat{d}_m^\dagger (\hat{d}_m) and \hat{c}_k^\dagger (\hat{c}_k) are creation (annihilation) operators of electron in state m on the molecule and state

k in the contact, respectively, and \hat{a}_{α}^\dagger (\hat{a}_{α}) are creation (annihilation) operators of photons in optical mode α .

The calculation of Raman scattering is facilitated by distinguishing between the incoming (or pumping) mode i and the set of final (or accepting) modes $\{f\}$ of the radiation field. The former is assumed to be populated by one photon, and only processes of in-scattering from this mode into the system are considered (that is, back action of the molecule onto this mode is disregarded). The latter are empty modes of the field: population flux into these modes is monitored by the measuring device, but they do not act back on the system, i.e., only out-scattering from the system into these modes is taken into account.

In Refs. 76,77 we have distinguished between ‘normal’ and ‘inverse’ Raman processes according to whether the molecule is initially in the ground or in the excited states. The latter occurrence is possible in a strongly biased junction. Here we consider only ‘normal’ Raman processes. The corresponding expression for the flux from the incoming mode i to outgoing mode f representing light scattering from the molecular junction at steady state was obtained in Ref. 77 (see Eq.(28) there):

$$J_{i \rightarrow f}^{(nR)} = \frac{|U_i|^2 |U_f|^2}{\hbar^4} \int_{-\infty}^{+\infty} d(t-t') \int_{-\infty}^t dt_1 \int_{-\infty}^{t'} dt_2 e^{i\nu_f(t-t')} e^{-i\nu_i(t_1-t_2)} \langle \hat{D}(t_2) \hat{D}^\dagger(t') \hat{D}(t) \hat{D}^\dagger(t_1) \rangle \quad (7)$$

where

$$\hat{D} = \hat{d}_1^\dagger \hat{d}_2 \quad (8)$$

is the molecular de-excitation operator. Note that generalized Franck-Condon factors that appear in Eq.(28) of Ref. 77 are omitted in Eq.(7) since we do not consider vibrational transitions.

Eq.(7) is already of the lowest needed (4th) order in the molecule-radiation field interaction, so to this order this interaction is disregarded in evaluating the four-time correlation function in the integrand. Substituting (8) into (7), applying Wick’s theorem,¹¹⁹ and assuming that energy separation between the two molecular levels is much larger than their broadening due to hybridization with metal state (this makes it possible to disregard non-diagonal elements of the single-electron Green function that describe the molecule in the junction) leads to (see appendix A for more details)

$$J_{\nu_i \rightarrow \nu_f} = \frac{2\pi}{\hbar} |U_i|^2 |U_f|^2 \rho(\nu_i) \rho(\nu_f) \{ \delta(\hbar\nu_i - \hbar\nu_f) \times \left| \int \frac{dE^{(1)}}{2\pi} \int \frac{dE^{(2)}}{2\pi} \frac{G_2^>(E^{(2)}) G_1^<(E^{(1)})}{\hbar\nu_i + E^{(1)} - E^{(2)} + i\delta} \right|^2 \quad (9a)$$

$$+ \int \frac{dE_i^{(1)}}{2\pi} \int \frac{dE_f^{(1)}}{2\pi} \delta(\hbar\nu_i + E_i^{(1)} - \hbar\nu_f - E_f^{(1)}) \quad (9b)$$

$$\times G_1^<(E_i^{(1)}) G_1^>(E_f^{(1)}) \left| \int \frac{dE^{(2)}}{2\pi} \frac{G_2^>(E^{(2)})}{\hbar\nu_i + E_i^{(1)} - E^{(2)} + i\delta} \right|^2$$

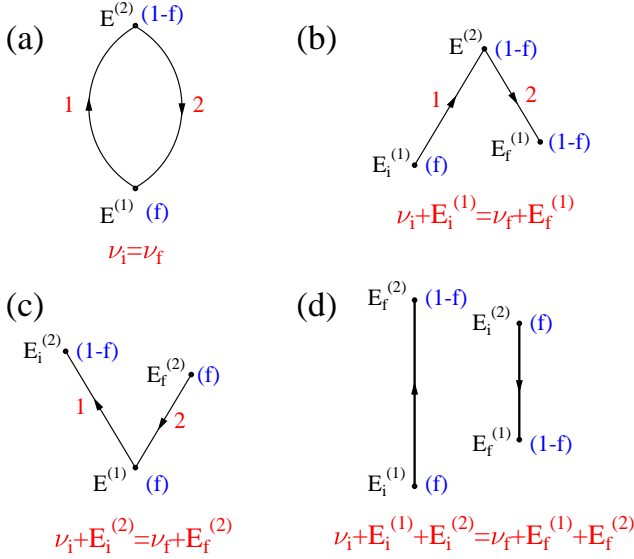


FIG. 2: (Color online) Sketch of electronic scattering events corresponding to expressions in Eq.(9). Shown are Rayleigh (a) and three types of electronic Raman scattering events (b)-(d). In (a) the light scattering process may be accompanied by an electron that goes from a state of energy $E^{(1)}$ to a state of energy $E^{(2)}$ then returns to the same state $E^{(1)}$, which involves twice the Fermi factors $f(E^{(1)}) (1 - f(E^{(2)}))$ as seen in Eq.(9a). In (b) the scattering process is accompanied by an electron starting from a state of energy $E_i^{(1)}$ and ending in state $E_f^{(1)}$ (hence the appearance of the Fermi product $f(E_i^{(1)}) (1 - f(E_f^{(1)}))$ in Eq.(9b)), having gone through a state of intermediate state of energy $E^{(2)}$ which can contribute if empty (implying the square of the corresponding Fermi factor, $(1 - f(E^{(2)}))^2$). In (c) the inelastic contribution results from an electron going from a state of energy $E_i^{(1)}$ to energy $E_i^{(2)}$ while another electron goes from energy $E_f^{(2)}$ to fill back the hole formed in $E_i^{(1)}$. This involves the occupation probability product $f(E_i^{(1)})^2 (1 - f(E_i^{(2)})) f(E_f^{(2)})$. Finally, process (d) results from two independent electronic transitions: The destruction of the incoming photon is accompanied by an electron moving from $E_i^{(1)}$ to $E_f^{(1)}$ while the creation of the outgoing photon is accompanied by an electron going from state $E_i^{(2)}$ to state $E_f^{(1)}$.

$$\begin{aligned}
& + \int \frac{dE_i^{(2)}}{2\pi} \int \frac{dE_f^{(2)}}{2\pi} \delta(\hbar\nu_i + E_i^{(2)} - \hbar\nu_f - E_f^{(2)}) \quad (9c) \\
& \times G_1^<(E_i^{(2)}) G_2^>(E_f^{(2)}) \left| \int \frac{dE^{(1)}}{2\pi} \frac{G_1^<(E^{(1)})}{\hbar\nu_i + E^{(1)} - E_f^{(2)} + i\delta} \right|^2
\end{aligned}$$

$$\begin{aligned}
& + \int \frac{dE_i^{(1)}}{2\pi} \int \frac{dE_f^{(1)}}{2\pi} \int \frac{dE_i^{(2)}}{2\pi} \int \frac{dE_f^{(2)}}{2\pi} \\
& \times \delta(\hbar\nu_i + E_i^{(1)} + E_i^{(2)} - \hbar\nu_f - E_f^{(1)} - E_f^{(2)}) \quad (9d) \\
& \times \left. \frac{G_1^<(E_i^{(1)}) G_1^>(E_f^{(1)}) G_2^<(E_i^{(2)}) G_2^>(E_f^{(2)})}{|\hbar\nu_i + E_i^{(1)} - E_f^{(2)} + i\delta|^2} \right\}
\end{aligned}$$

where $G_m^{>,<}(E)$ ($m = 1, 2$) are greater and lesser projections of the single-particle Green function

$$G_m^>(E) = -i \sum_{K=L,R} \frac{\Gamma_m^K [1 - f_K(E)]}{(E - \varepsilon_m)^2 + (\Gamma_m/2)^2} \quad (10)$$

$$G_m^<(E) = i \sum_{K=L,R} \frac{\Gamma_m^K f_K(E)}{(E - \varepsilon_m)^2 + (\Gamma_m/2)^2} \quad (11)$$

and where

$$\Gamma_m^K(E) \equiv 2\pi \sum_{k \in K} |V_{km}|^2 \delta(E - \varepsilon_k) \quad (K = L, R) \quad (12)$$

are electron escape rates from molecular level m into contact K , and $\Gamma_m \equiv \sum_{K=L,R} \Gamma_m^K$. In general the parameter δ should be replaced by broadening of the optical signal due to interaction with environment. The latter is not included in the model explicitly, i.e. within the model $\delta \rightarrow 0+$. The notation used for the integration variables in Eqs.(9) is chosen to help the physical interpretation of the different contributions to the scattering signal: we use the upper indices (1) or (2) to mark the molecular origin (molecular states 1 or 2) of the electronic optical transitions (in our model electrons interact with light through their interaction with the molecule), while lower indices i and f mark initial and final states of the scattering process.

The scattering flux (9) is seen to include four contributions: Rayleigh scattering, Eq.(9a), and three types of electronic Raman scattering processes, Eqs. (9b)-(9d). In the following we are interested in Raman scattering only. Eqs. (9b) and (9c) represent electronic Raman scattering with initial and final metal electronic states near the ground ($m = 1$) and excited ($m = 2$) states of the molecule, respectively. Eq.(9d) corresponds to coherent two-electron Raman scattering event with electrons starting in both ground and excited states of the molecule. The processes are sketched in Figure 2. The Fermi occupations involved in these expressions imply that at zero bias and low temperature processes (b) or (c) dominate if, respectively, levels 1 or 2 is closer to the Fermi energy, while process (d) can contribute only weakly since it requires that both levels 1 and 2 couple to occupied and non-occupied metal states. For highly biased junctions all processes can contribute as will be seen below.

III. HEATING OF THE ELECTRONIC DISTRIBUTION

Standard theories of molecular conduction are based on the Landauer theory that assumes that electrons entering the junction reflect the Fermi distribution of their reservoir of origin. At the same time, Landauer theory assumes that thermal relaxation of the transmitted charge takes place only in the interior of the electrode. Obviously, in a current carrying junction, a small region near the metal-molecule contact will be characterized by different distributions for the electrons moving toward the junction and away from it. The electronic distribution as a function of energy and position in this region depends on the relaxation processes associated with electron-electron and electron phonon interactions. A simple model that addresses this issue was discussed in Ref. 86. Here we assume that the electronic distribution in the electrodes contact regions that contribute to the inelastic light scattering signal through their interaction with the molecular bridge is dominated by the transmission process, and that thermal relaxation can be disregarded in these regions. Obviously, a heating estimate based on this assumption is an upper bound to the actual heating. Denoting the junction transmission coefficient by $T(E)$ and the equilibrium Fermi distributions in the left and right electrodes by $f_K(E)$; $K = L, R$, the steady state electronic distributions in these contact regions are

$$\begin{aligned} f_L^{SS}(E) &= \frac{1}{2} [f_L(E) + (1 - T(E)) f_L(E) + T(E) f_R(E)] \\ &= f_L(E) + \frac{1}{2} T(E) [f_R(E) - f_L(E)] \end{aligned} \quad (13a)$$

$$f_R^{SS}(E) = f_R(E) + \frac{1}{2} T(E) [f_L(E) - f_R(E)] \quad (13b)$$

It is a common practice to associate an effective temperature with a given non-equilibrium distribution. Usually it is done by fitting the distribution to the corresponding equilibrium expression, that is using (13) to define effective temperatures according to

$$f_K^{SS}(E) = \frac{1}{e^{(E - \mu_K)/k_B T_K^{eff}} + 1}; \quad K = L, R \quad (14)$$

However, this procedure is inadequate, since the distributions (13) can be very different from a Fermi function. Instead we define the effective temperature by the requirement that a weak contact between our non-equilibrium system and an equilibrium system characterized by the desired effective temperature and the same electrochemical potential (μ_L or μ_R) carries no heat current. This implies the following definition of the effective temperature:

$$\int \frac{dE}{2\pi} (E - \mu_K) [f_K^{SS}(E) - f_K(E, T_K^{eff})] = 0 \quad (15)$$

For energy independent transmission, the distributions (13) are characterized by excess holes below the Fermi energy of the lower voltage side and excess electrons above

the Fermi energy on the higher voltage side, both amount to heating, i.e. $T_K^{eff} > T$. It should be emphasized, however, that the non-equilibrium junction cannot be really characterized by a single effective temperature. For energy dependent transmission heating is not the same on both sides, and can in fact become cooling on one side. This limitation of the effective temperature concept will become evident also when we compare in the next section the “effective temperature” obtained from the electronic contribution to inelastic light scattering to that associated with Eqs. (13).

IV. RESULTS: THE RAMAN CONTINUUM AND ITS “EFFECTIVE TEMPERATURE” IN BIASED MOLECULAR CONDUCTION JUNCTIONS

In what follows we present results of model calculations of the Raman continuum in equilibrium and in biased molecular conduction junctions, evaluate the heating associated with the current flow through the biased junction and compare the effective temperature extracted from the light scattering signal to that associated with the non-equilibrium distributions (13). Unless otherwise stated, we have used the junction model described in Section II and Figure 1 with the following set of parameters: The Fermi energy (electrochemical potential) in the unbiased junction is taken zero, and the molecular levels are placed at $E_1 = -1.5$ eV and 1.0 eV. The potential bias V_{sd} is assumed to divide symmetrically between the two contacts, so the electrochemical potentials under bias are $\mu_L = |e|V_{sd}/2$ and $\mu_R = -|e|V_{sd}/2$ (e is the electronic charge). The incident frequency is taken $\hbar\nu_i = 1.5$ eV. The molecule-metal coupling is measured by the widths Γ_m^K ; $m = 1, 2$; $K = L, R$. These four parameters are all taken to be 0.25 eV in a symmetric junction. We have also examined junction asymmetry, e.g., when one of the leads is an STM tip, taking in this case $\Gamma_m^L = 0.25$ eV and $\Gamma_m^R = 0.0025$ eV for both molecular levels. The width parameter δ in Eq.(9) should reflect environmental broadening, and is taken 0.01 eV. Finally, we examine the system behavior at two temperatures, $T = 0, 300$ K. All energy integrations are done on a grid of 3001 points distributed uniformly in the interval $-3.0 \dots 3.0$ eV.

Figures 3 show the effective electronic temperatures calculated from Eq.(15) with these model parameters. Figs. 3a and 3b show results for the symmetric, $\Gamma^L = \Gamma^R$, and asymmetric, $\Gamma^L \neq \Gamma^R$ junctions as detailed above, and Fig. 3c shows results obtained from a junction characterized by a simple square barrier of height 5 eV and width 3 Å. Obviously, the temperatures calculated for the left and right leads are not equal and their difference increases with voltage as the effect of the energy dependence of the transmission coefficient becomes more pronounced. Note that the main difference between the results in (a) and (b) is not related to the junction asymmetry but simply to the fact that, with the parameters

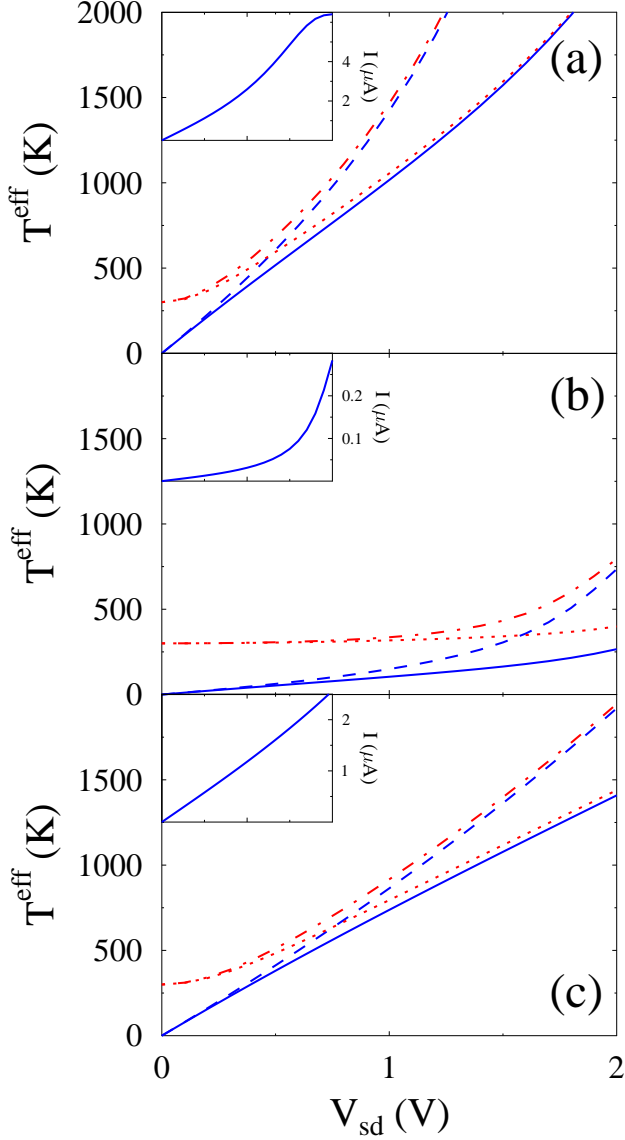


FIG. 3: (Color online) (a) The effective temperatures, Eq.(15), calculated for symmetric junctions with ambient temperatures $T = 0$ K and 300 K. The blue full and dashed lines show respectively the left and right electronic temperatures for the case $T = 0$ K. The red dotted and dashed dotted lines are similar results for $T = 300$ K. The inset shows the corresponding I/V curves, for which the $T = 0$ K and $T = 300$ K results overlap. (b) Same results for the asymmetric junction case. (c) Similar results for a tunneling junction characterized by a square barrier of height 5 eV (above the Fermi energy of the unbiased junction) and width 3 Å.

chosen, the asymmetric junction carries a much smaller current. Note also that the results for the $T = 0$ K and $T = 300$ K cases converge at high voltage. Finally, it should be kept in mind that these results represent an upper bound on the electronic heating, since thermal relaxation of the electron gas was disregarded.

Figures 4 show the electronic contribution to the in-

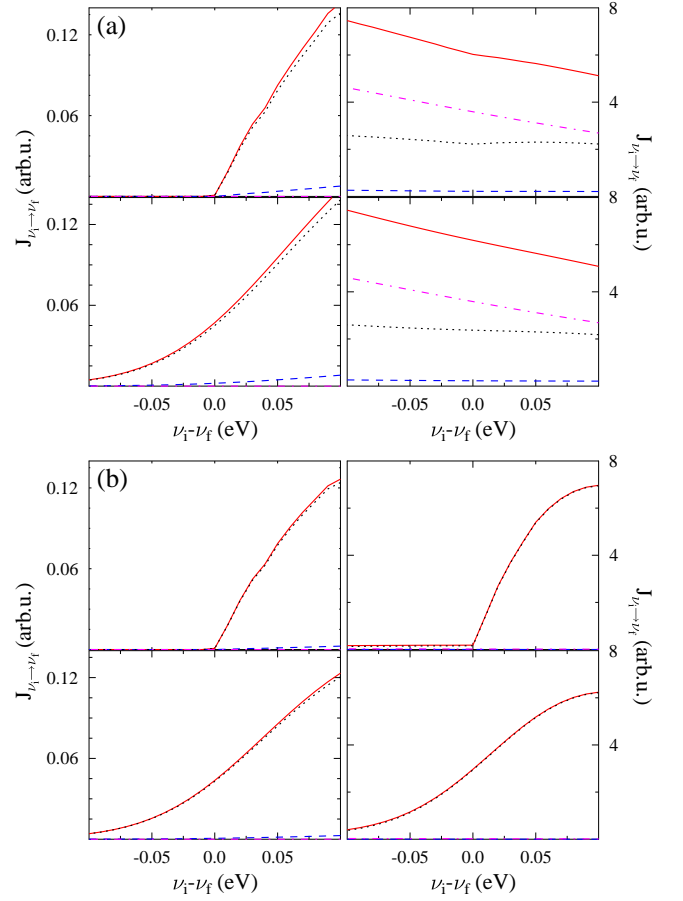


FIG. 4: (Color online) (a) The electronic Raman intensity, $J_{\nu_i \rightarrow \nu_f} \sim J_{i \rightarrow f} \nu_f^3$, calculated for the symmetric junction, $\Gamma_m^L = \Gamma_m^R = 0.25$; $m = 1, 2$, displayed as function of the Raman shift $\nu_i - \nu_f$ for $V_{\text{sd}} = 0$ (left panels) and $V_{\text{sd}} = 2$ V (right panels) and for ambient temperatures $T = 0$ K (upper panels) and $T = 300$ K (lower panels). The solid (red) line shows the overall light scattering intensity while the other lines correspond to the different contributions: Eqs. (9b) (dashed, blue), (9c) (dotted, black) and (9d) (dash-dotted, magenta). (b) Same as Fig. 4a, for the asymmetric junction, $\Gamma_m^L = 0.25$ eV, $\Gamma_m^R = 0.0025$ eV; $m = 1, 2$.

elastic light scattering signal calculated for our model. Several observations are noteworthy: First, the equilibrium (zero bias) signal is dominated by the contribution (9c) because the upper molecular level 2 lies closer to the Fermi energy than the lower level 1. (From (9b) and (9c) it follows that the relative magnitudes of these terms go like $(1 - f_1)(1 - f_2)$ and $f_1 f_2$, respectively). When the bias increases, the electrochemical potential of the left lead approaches level 2, and, more importantly, that of the right lead comes closer to level 1, whereas contributions (9b) and (9d) that require finite hole population near level 1 also become important. For high enough bias, contribution (9d), which requires partially populated metal electronic states near both levels 1 and 2, can become the most significant, as seen in the right panels

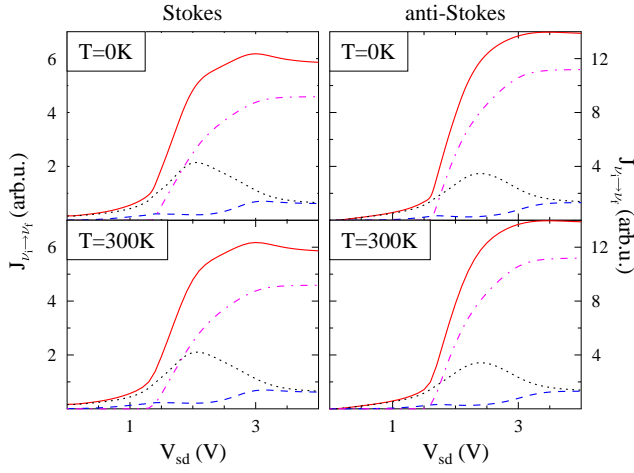


FIG. 5: (Color online) The electronic Raman intensity for $|\nu_i - \nu_f| = 0.125$ eV shown as a function of the bias potential for the symmetric junction, $\Gamma_m^L = \Gamma_m^R = 0.25$ eV, $m = 1, 2$. Line notations are as in Fig. 4.

of Fig. 4a. This is not seen in the corresponding panels of the asymmetric case, Fig. 4b, because although level 1 is approached by the electrochemical potential of the right lead, the corresponding hole population near this level is essentially unaffected because of the very weak right electrode - molecule coupling. Second, when process (9d) become important, the anti-Stokes signal may exceed the Stokes intensity as seen in the right panels of Fig. 4a. In this case the “effective temperature” associated with the electronic Raman scattering becomes meaningless. We return to this issue below.

The results shown in Figs. 4 emphasize the importance of the relative positions of the relevant molecular levels with respect to the left and right chemical potentials in determining the light scattering signal as a function of the frequency shift and bias. This is seen also in Figures 5 where the Raman signal is displayed against the bias potential. We see again that the electronic inelastic light scattering is dominated by different contributions at low and high bias and that the anti-Stokes signal can exceed the Stokes at high bias.

As in the Raman shift plots shown in Figs 4, also the voltage dependence depicted in Figures 5 reflects mainly the strong energy dependence of the Fermi functions appearing in Eqs. (9)-(11). This sensitivity suggests that attempts to characterize the junction temperature from the Stokes and anti-Stokes signals should be regarded with caution. This is made evident by comparing Figures 6 and 3. Fig. 6 depicts the “Raman effective temperature”, $T_{S/AS}^{eff}$ obtained from the Stokes-anti-Stokes intensities ratio according to

$$T_{S/AS}^{eff} = \frac{\Delta\nu}{\ln \left(\frac{J_{\nu_i \rightarrow \nu_i - \Delta\nu}}{J_{\nu_i \rightarrow \nu_i + \Delta\nu}} \times \frac{(\nu_i + \Delta\nu)^3}{(\nu_i - \Delta\nu)^3} \right)} \quad (16)$$

and plotted against the Raman shift. Independence of

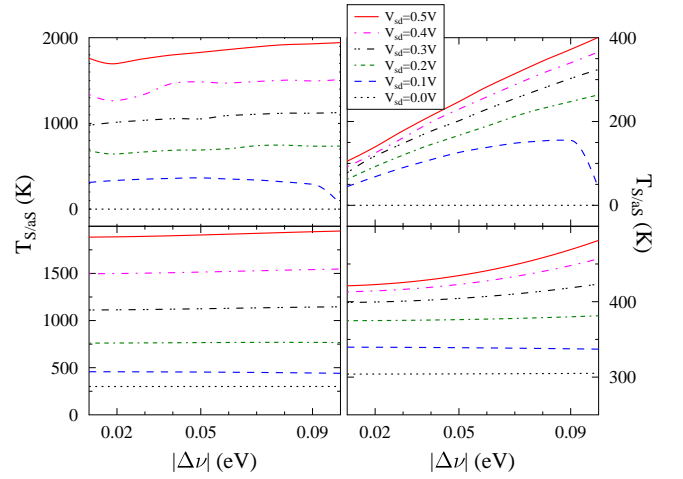


FIG. 6: (Color online) The effective Raman temperature estimated from the Stokes/anti-Stokes ratio of the electronic Raman spectrum, plotted as a function of the inelastic shift for different voltage biases. Left and right panels show results for the symmetric and asymmetric junctions as defined by the choice of the Γ parameters. Upper and lower panels correspond to ambient temperatures $T = 0$ K and $T = 300$ K, respectively.

$T_{S/AS}^{eff}$ on the Raman shift is a prerequisite for a meaningful effective temperature, and this is indeed satisfied approximately for all cases displayed in Fig. 6 except for the asymmetric junction at low ambient temperature. As pointed out above, this apparently simple picture breaks down at higher voltages, where the S/AS ratio can become smaller than 1 and using Eq.(16) for temperature estimate is unfeasible. It should be emphasized that the Raman temperature calculated according to Eqs. (9)-(11) and (16) is found to be in excellent agreement with the imposed ambient temperature at equilibrium.¹¹⁷ However, at least for high bias, the information embedded in the inelastic scattering continuum cannot be described by a useful Raman ‘effective temperature’, although it certainly shows evidence of electronic heating in the biased junction.

Even in the low voltage regime shown in Figure 6, the temperatures estimated from Eq.(16) are significantly higher than those obtained directly from the steady-state electronic distribution, Eq.(15), which was argued above to constitute an upper bound to the actual heating. The fact that the Raman temperature implies heating that is considerably larger than what can be associated directly with the electronic distribution in the metals suggests that its origin lies elsewhere.

We have considered this origin in a recent short publication.¹¹⁷ An important feature of our model is the assumption that the interaction between the junction and the radiation field that give rise to the Raman scattering originates from that between the molecular bridge and the radiation field. This implies that although the Raman signal discussed here is associated with electronic

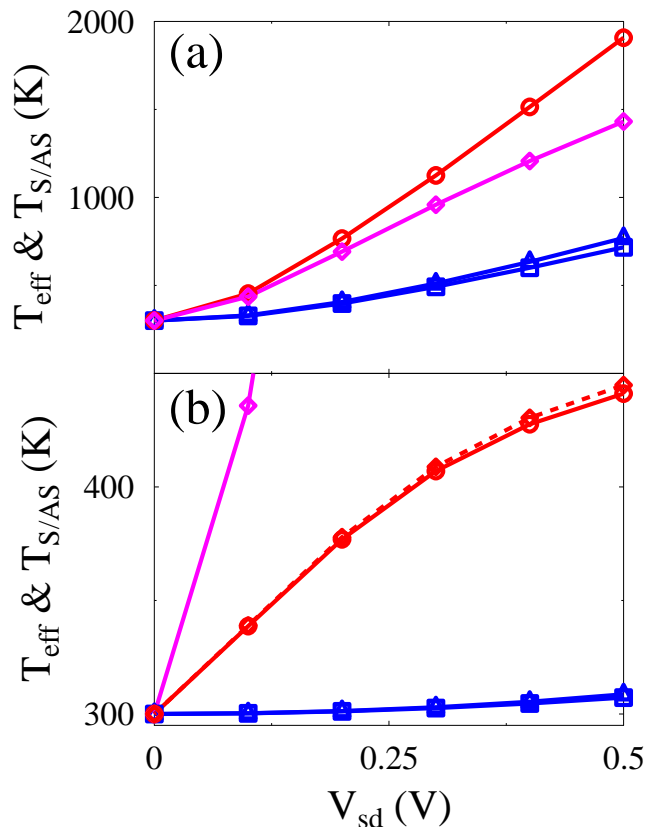


FIG. 7: (Color online) Non-equilibrium effective temperatures at low bias, $|e|V_{sd} = \mu_L - \mu_R \ll \varepsilon_2 - \varepsilon_1$. The bias is applied symmetrically, $\mu_L = |e|V_{sd}/2$ and $\mu_R = -|e|V_{sd}/2$. Both panels compare the Raman temperature (circles, red), Eq.(16), and the effective electronic temperatures of contacts L (triangles, blue) and R (squares, blue) obtained from Eq.(15) displayed against the voltage bias. Note that these estimates (magenta lines) overlap in panel (a). In panel (a) (reproduced from Ref. 117) we consider the symmetric junction, $\Gamma_m^L = \Gamma_m^R = 0.25$ eV for both molecular states. Panel (b) shows results for the asymmetric junction, $\Gamma_m^L = 0.25$ and $\Gamma_m^R = 0.0025$ eV. The electronic Raman temperature was calculated both for leads at thermal equilibrium ($T = 300$ K) and for leads characterized by the distributions (13). The results are identical in the symmetrical case and are almost indistinguishable also in the asymmetric system (full and dashed red lines in panel (b)). Two effective molecular electronic temperatures: one defined in Eq.(17) (diamonds, magenta) and another defined in Eq.(18) (asterisks, magenta).

transitions in the metal, the coupling to the radiation field results from the metal-molecule interaction; therefore the calculated scattering may be affected by the electronic non-equilibrium in the molecule.

To examine the possible significance of this effect we have attempted to estimate the effective electronic temperature T_M of the non-equilibrium molecule in two ways. One (already presented in our recent publication¹¹⁷ uses

an analog of Eq.(15)

$$\int \frac{dE}{2\pi} (E - \mu_M) \sum_{m=1,2} (f(E, \mu_M, T_M) G_m^>(E) + [1 - f(E, \mu_M, T_M)] G_m^<(E)) = 0 \quad (17)$$

which represents the condition that the heat current between the molecule and a fictitious equilibrium free electron bath, characterized by the same chemical potential μ_M and the effective temperature T_M , vanishes.^{86,117} While the physics behind Eq.(17) is clear, its weakness lies in the fact that the chemical potential μ_M is not well defined. As in Ref. 117 we use a heuristic extension of the equilibrium expression $\mu = (\partial E / \partial n)$ to obtain, for a steady state characterized by given electron and energy fluxes, J_E and J_e , respectively, $\mu_M = \frac{dE}{dn} / \frac{dn}{dt} = J_E / J_e$ where n is the number of electrons on the molecule. Both J_E and J_e are easily obtained from the Landauer theory.⁸⁶

Alternatively, effective molecular electronic temperature and chemical potential can be defined as the temperature and the chemical potential of an equilibrium Fermi bath coupled to the non-equilibrium molecule, determined such that both particle and energy fluxes between them vanish

$$\int \frac{dE}{2\pi} \sum_{m=1,2} (f(E, \mu_M, T_M) G_m^>(E) + [1 - f(E, \mu_M, T_M)] G_m^<(E)) = 0 \quad (18a)$$

$$\int \frac{dE}{2\pi} E \sum_{m=1,2} (f(E, \mu_M, T_M) G_m^>(E) + [1 - f(E, \mu_M, T_M)] G_m^<(E)) = 0 \quad (18b)$$

Eqs. 18 were solved for the unknowns T_M and μ_M by an iterative procedure.

Figures 7 show the results of these calculations. The Raman temperature, Eq.(16), is compared to the effective electronic temperatures of the two leads, obtained from Eq.(15) and to the molecular effective electronic temperatures calculated from Eqs. (17) and (18). Note that Section III implies that the Raman temperature should be calculated using the non-equilibrium distributions (13), however the low bias results are almost indistinguishable from those obtained using the equilibrium Fermi-Dirac distributions. In fact, for the symmetric junction, $\Gamma^L = \Gamma^R$, the results are identical for any bias. To see this note that the lesser and greater Green functions that enter in the Raman signal have the forms $G^<(E) = i|G^r(E)|^2[\Gamma^L f_L(E) + \Gamma^R f_R(E)]$; $G^>(E) = -i|G^r(E)|^2[\Gamma^L(1 - f_L(E)) + \Gamma^R(1 - f_R(E))]$, which, for $\Gamma^L = \Gamma^R$ are not sensitive to the difference between $f_K^S(E)$ and $f_K^{eq}(E)$ ($K = L, R$).

While all steady-state temperature estimates shown in Fig. 7 indicate heating, the molecular electronic temperature is seen to be considerably higher than the effective temperature that characterizes the electronic distributions in the leads at the leads-molecule interfaces.

The most significant observation is that the Raman electronic temperature is also considerably higher than that of the metal leads, and seems to reflect the behavior of the molecular electronic distribution. In the symmetric junction case the Raman and the molecular estimates are seen to be quite close for both definitions of the latter, Eqs. (17) and (18). For the asymmetric junction agreement is considerably worse, however the Raman temperature is bound by the two molecular estimates. More than anything, these estimates show that there is no unique reliable way to define effective temperature in non-equilibrium system. Still, both estimates of the molecular electronic temperature are considerably higher than the effective electronic temperature of the metals and are closer to the Raman temperature. The Raman measure is of course unique and well defined, but apart from giving general indication of heating, it does not quantitatively reflect the actual heating in the metal. Obviously, the observed Raman electronic temperature cannot be taken as a direct estimate of the leads heating.

V. SUMMARY AND CONCLUSIONS

In this paper we have advanced a new approach for the description of the electronic background continuum in Raman scattering from molecules adsorbed on metal surfaces. This approach, based on the non-equilibrium Green function technique, makes it possible to generalize the theory to non-equilibrium situations, and we have applied it to discuss the background Raman scattering from molecular conduction junctions. We obtained (under the simplification that focuses on the vibrationless part of the Raman spectrum) an explicit expression, Eq.(9) for the electronic Raman background in terms of the non-equilibrium electronic distributions in the leads. These distributions, Eqs.(13), were obtained from scattering theory considerations under the assumption that electronic relaxation can be disregarded in the contact regions that contribute to the electronic Raman signal. Using together the new theory of the Raman background and our estimate for the non-equilibrium electronic distribution at the metal-molecule contact, we were able to analyze non-equilibrium effects in the junction Raman scattering.

As a particular application of our theory we have considered the heating caused by electronic conduction through the junction. This heating can be monitored through the ratio between the Stokes (S) and anti-Stokes (AS) Raman signal. Standard theories of molecular conduction junctions assume that the metal leads maintain their equilibrium temperature in the conducting steady state of a biased junction, however recent experimental results¹² suggest that heating of the electronic distribution near the molecule-metal contact does take place. Our results indicate that: (a) The electronic Raman scattering, namely the Raman continuous background, indeed contain information about electronic heating in the

metal-molecule contact region; (b) The Raman temperature is considerably higher than an upper bound estimated from the (generally energy dependent) junction transmission coefficient. (c) The Raman temperature reflects the non-equilibrium nature of the molecular bridge more than that of the electronic distributions in the leads. (d) While the non-equilibrium Raman scattering signal can always be calculated from Eq.(9), the Raman temperature, Eq.(16), becomes meaningless at high bias, when the AS signal may surpass the S one.

In conclusion, recent experimental work has shown that Raman scattering can be a very useful probe of non-equilibrium molecular conduction junctions, however theoretical analysis is sometimes necessary for the correct interpretation of observations and their significance.

Acknowledgments

AN's research is supported by the Israel Science Foundation, the Israel-US Binational Science Foundation, the European Science Council (FP7/ERC grant no. 226628) and the IsraelNiedersachsen Research Fund. MG gratefully acknowledges support by the DOE (Early Career Award, DE-SC0006422), the NSF (CHE-1057930), the BSF (2008282), and the Hellmann Family Foundation. We thank Doug Natelson for bringing up the issue of electronic temperature in biased junctions and for sharing his data prior to publication, and Mark Ratner for many helpful discussions.

Appendix A: Derivation of Eq.(9)

Using Eq.(8) in the expression for the Raman flux, Eq.(7), one gets a multi-time correlation function of the form $\langle \hat{d}_1^\dagger(t_2)\hat{d}_2(t_2)\hat{d}_2^\dagger(t')\hat{d}_1(t')\hat{d}_1^\dagger(t)\hat{d}_2(t)\hat{d}_2^\dagger(t_1)\hat{d}_1(t_1) \rangle$. The time evolution here is governed by the junction Hamiltonian $\hat{H}_M + \hat{H}_K + \hat{V}_{KM}$, Eqs. (2)-(4), so Wicks theorem can be used. Assuming that the separation between molecular levels 1 and 2 is much larger than their broadening, i.e., neglecting inter-level correlations associated with the molecule-metal interaction, leads to

$$\begin{aligned} \langle \hat{d}_1^\dagger(t_2)\hat{d}_2(t_2)\hat{d}_2^\dagger(t')\hat{d}_1(t')\hat{d}_1^\dagger(t)\hat{d}_2(t)\hat{d}_2^\dagger(t_1)\hat{d}_1(t_1) \rangle = \\ [G_1^<(t_1 - t_2)G_1^>(t' - t) - G_1^<(t' - t_2)G_1^<(t_1 - t)] \times \\ [G_2^>(t_2 - t_1)G_2^<(t - t') - G_2^>(t_2 - t')G_2^>(t - t_1)] \quad (\text{A1}) \end{aligned}$$

where $G_m^>(t - t') = -i \langle \hat{d}_m(t)\hat{d}_m^\dagger(t') \rangle$ and $G_m^<(t - t') = i \langle \hat{d}_m^\dagger(t')\hat{d}_m(t) \rangle$, ($m = 1, 2$). Eqs. (10)-(11) are the Fourier transforms of these correlation functions. Using Eq.(A1) in (7) and expressing all correlation functions in terms of their Fourier transforms leads to the four terms of Eq.(9).

- * Electronic address: migalperin@ucsd.edu
- † Electronic address: nitzan@post.tau.ac.il
- ¹ A. M. Michaels, J. Jiang, and L. Brus, *J. Phys. Chem. B* **104**, 11965 (2000).
 - ² J. Jiang, K. Bosnick, M. Maillard, and L. Brus, *J. Phys. Chem. B* **107**, 9964 (2003).
 - ³ J. H. Tian, B. Liu, X. L. Li, Z. L. Yang, B. Ren, S. T. Wu, N. J. Tao, and Z. Q. Tian, *J. Am. Chem. Soc.* **128**, 14748 (2006).
 - ⁴ D. R. Ward, N. K. Grady, C. S. Levin, N. J. Halas, Y. Wu, P. Nordlander, and D. Natelson, *Nano Lett.* **7**, 1396 (2007).
 - ⁵ J. P. Camden, J. A. Dieringer, Y. M. Wang, D. J. Masiello, L. D. Marks, G. C. Schatz, and R. P. Van Duyne, *J. Am. Chem. Soc.* **130**, 12616 (2008).
 - ⁶ X. Chen, S. Yeganeh, L. Qin, S. Li, C. Xue, A. B. Braunschweig, G. C. Schatz, M. A. Ratner, and C. A. Mirkin, *Nano Lett.* **9**, 3974 (2009).
 - ⁷ H. C. C. Pedro and et al., *Nanotechnology* **20**, 434020 (2009).
 - ⁸ W. Li, P. H. C. Camargo, X. Lu, and Y. Xia, *Nano Lett.* **9**, 485 (2009).
 - ⁹ M. Rycenga, P. H. C. Camargo, W. Y. Li, C. H. Moran, and Y. Xia, *J. Phys. Chem. Lett.* **1**, 696 (2010).
 - ¹⁰ K. L. Wustholz, A. I. Henry, J. M. McMahon, R. G. Freeman, N. Valley, M. E. Piotti, M. J. Natan, G. C. Schatz, and R. P. Van Duyne, *J. Am. Chem. Soc.* **132**, 10903 (2010).
 - ¹¹ D. R. Ward, N. J. Halas, J. W. Ciszek, J. M. Tour, Y. Wu, P. Nordlander, and D. Natelson, *Nano Lett.* **8**, 919 (2008).
 - ¹² D. R. Ward, D. A. Corley, J. M. Tour, and D. Natelson, *Nat Nano* **6**, 33 (2011).
 - ¹³ Z. Ioffe, T. Shamai, A. Ophir, G. Noy, I. Yutsis, K. Kfir, O. Cheshnovsky, and Y. Selzer, *Nature Nanotech.* **i3**, 727 (2008).
 - ¹⁴ An alternative electronic origin of such correlations was recently suggested by Park and Galperin.^{15,16}
 - ¹⁵ T.-H. Park and M. Galperin, *Europhys. Lett.* **95**, 27001 (2011).
 - ¹⁶ T.-H. Park and M. Galperin, *Phys. Rev. B* **84**, 075447 (2011).
 - ¹⁷ H. P. Yoon, M. M. Maitani, O. M. Cabarcos, L. Cai, T. S. Mayer, and D. L. Allara, *Nano Lett.* **10**, 2897 (2010).
 - ¹⁸ S. Grafstrom, *J. Appl. Phys.* **91**, 1717 (2002).
 - ¹⁹ E. Flaxer, O. Sneh, and O. Cheshnovsky, *Science* **262**, 2012 (1993).
 - ²⁰ K. Sakamoto, K. Meguro, R. Arafune, M. Satoh, Y. Uehara, and S. Ushioda, *Surf. Sci.* **502**, 149 (2002).
 - ²¹ X. H. Qiu, G. V. Nazin, and W. Ho, *Science* **299**, 542 (2003).
 - ²² Smolyaninov, II, *Surf. Sci.* **364**, 79 (1996).
 - ²³ D. Fujita, T. Ohgi, W. L. Deng, H. Nejo, T. Okamoto, S. Yokoyama, K. Kamikado, and S. Mashiko, *Surf. Sci.* **454**, 1021 (2000).
 - ²⁴ W. Deng, D. Fujita, T. Ohgi, S. Yokoyama, K. Kamikado, and S. Mashiko, *J. Chem. Phys.* **117**, 4995 (2002).
 - ²⁵ Z. C. Dong, et al., *Jap. J. Appl. Phys. Part 1* **41**, 4898 (2002).
 - ²⁶ Z. C. Dong, A. S. Trifonov, X. L. Guo, K. Amemiya, S. Yokoyama, T. Kamikado, T. Yamada, S. Mashiko, and T. Okamoto, *Surf. Sci.* **532**, 237 (2003).
 - ²⁷ X. L. Guo, Z. C. Dong, A. S. Trifonov, S. Yokoyama, S. Mashiko, and T. Okamoto, *Jap. J. Appl. Phys. Part 1* **42**, 6937 (2003).
 - ²⁸ X. L. Guo, Z. C. Dong, A. S. Trifonov, S. Yokoyama, S. Mashiko, and T. Okamoto, *Appl. Phys. Lett.* **84**, 969 (2004).
 - ²⁹ X.-L. Guo, Z.-C. Dong, A. S. Trifonov, K. Miki, Y. Wakayama, D. Fujita, K. Kimura, S. Yokoyama, and S. Mashiko, *Phys. Rev. B* **70**, 233204 (2004).
 - ³⁰ X.-L. Guo, Z.-C. Dong, A. S. Trifonov, S. Yokoyama, S. Mashiko, and T. Okamoto, *Appl. Phys. Lett.* **84**, 969 (2004).
 - ³¹ R. Nishitani, Y. Tateishi, H. Arakawa, A. Kasuya, and K. Sumiyama, *Acta Phys. Polon. A* **104**, 269 (2003).
 - ³² T.-H. Lee, J. I. Gonzalez, J. Zheng, and R. M. Dickson, *Acc. Chem. Res.* **38**, 534 (2005).
 - ³³ H. W. Liu, Y. Ie, R. Nishitani, Y. Aso, and H. Iwasaki, *Phys. Rev. B* **75**, 115429 (2007).
 - ³⁴ D. C. Guhr, D. Rettinger, J. Boneberg, A. Erbe, P. Leiderer, and E. Scheer, *Phys. Rev. Lett.* **99**, 086801 (2007).
 - ³⁵ N. Ittah, G. Noy, I. Yutsis, and Y. Selzer, *Nano Lett.* **9**, 1615 (2009).
 - ³⁶ G. Noy, A. Ophir, and Y. Selzer, *Angew. Chem. Int. Edit.* **49**, 5734 (2010).
 - ³⁷ D. R. Ward, F. Huser, F. Pauly, J. C. Cuevas, and D. Natelson, *Nat Nano* **5**, 732 (2010).
 - ³⁸ P. Banerjee, D. Conklin, S. Nanayakkara, T. H. Park, M. J. Therien, and D. A. Bonnell, *ACS Nano* **4**, 1019 (2010).
 - ³⁹ M. A. Mangold, M. Calame, M. Mayor, and A. W. Holleitner, *J. Am. Chem. Soc.* **133**, 12185 (2011).
 - ⁴⁰ S. Battacharyya, A. Kibel, G. Kodis, P. A. Liddell, M. Gervaldo, D. Gust, and S. Lindsay, *Nano Lett.* **11**, 2709 (2011).
 - ⁴¹ D. Dulic, S. J. van der Molen, T. Kudernac, H. T. Jonkman, J. J. D. de Jong, T. N. Bowden, J. van Esch, B. L. Feringa, and B. J. van Wees, *Phys. Rev. Lett.* **91**, 207402 (2003).
 - ⁴² T. Kudernac, S. J. van der Molen, B. J. van Wees, and B. L. Feringa, *Chem. Commun.*, 3597 (2006).
 - ⁴³ N. Katsonis, T. Kudernac, M. Walko, S. J. van der Molen, B. J. van Wees, and B. L. Feringa, *Adv. Mat.* **18**, 1397 (2006).
 - ⁴⁴ Y. Wakayama, K. Ogawa, T. Kubota, H. Suzuki, T. Kamikado, and S. Mashiko, *Appl. Phys. Lett.* **85**, 329 (2004).
 - ⁴⁵ S. Yasutomi, T. Morita, Y. Imanishi, and S. Kimura, *Science* **304**, 1944 (2004).
 - ⁴⁶ C. Zhang, M. H. Du, H. P. Cheng, X. G. Zhang, A. E. Roitberg, and J. L. Krause, *Phys. Rev. Lett.* **92**, 158301 (2004).
 - ⁴⁷ J. He, F. Chen, P. A. Liddell, J. Andréasson, S. D. Straight, D. Gust, T. A. Moore, A. L. Moore, J. Li, O. F. Sankey, and S. M. Lindsay, *Nanotechnology* **16**, 695 (2005).
 - ⁴⁸ S. W. Wu, N. Ogawa, and W. Ho, *Science* **312**, 1362 (2006).
 - ⁴⁹ I. Thanopoulos and E. Paspalakis, *Phys. Rev. B* **76**, 035317 (2007).
 - ⁵⁰ J. M. Mativetsky, G. Pace, M. Elbing, M. A. Rampi, M. Mayor, and P. Samori, *J. Am. Chem. Soc.* **130**, 9192 (2008).

- (2008).
- ⁵¹ S. J. van der Molen, J. Liao, T. Kudernac, J. S. Agustsson, L. Bernard, M. Calame, B. J. van Wees, B. L. Feringa, and C. Schönenberger, *Nano Lett.* **9**, 76 (2009).
 - ⁵² A. Levy Yeyati, A. Martin-Rodero, and F. Flores, *Phys. Rev. Lett.* **71**, 2991 (1993).
 - ⁵³ A. Tikhonov, R. D. Coalson, and Y. Dahnovsky, *J. Chem. Phys.* **117**, 567 (2002).
 - ⁵⁴ A. Tikhonov, R. D. Coalson, and Y. Dahnovsky, *J. Chem. Phys.* **116**, 10909 (2002).
 - ⁵⁵ S. Kohler, J. Lehmann, and P. Hänggi, *Phys. Rep.* **406**, 379 (2005), and references therein.
 - ⁵⁶ J. Lehmann, S. Kohler, V. May, and P. Hänggi, *J. Chem. Phys.* **121**, 2278 (2004).
 - ⁵⁷ J. M. Villas-Boas, A. O. Govorov, and S. E. Ulloa, *Phys. Rev. B* **69**, 125342 (2004).
 - ⁵⁸ T. Brandes, R. Aguado, and G. Platero, *Phys. Rev. B* **69**, 205326 (2004).
 - ⁵⁹ G. Zhou and Y. Li, *J. Phys.: Condens. Matter* **17**, 6663 (2005).
 - ⁶⁰ R. Lu and Z.-R. Liu, *J. Phys.: Condens. Matter* **17**, 5859 (2005).
 - ⁶¹ A. Keller, O. Atabek, M. Ratner, and V. Mujica, *J. Phys. B* **35**, 4981 (2002).
 - ⁶² I. Urdaneta, A. Keller, O. Atabek, and V. Mujica, *J. Phys. B* **38**, 3779 (2005).
 - ⁶³ I. Urdaneta, A. Keller, O. Atabek, and V. Mujica, *J. Chem. Phys.* **127**, 154110 (2007).
 - ⁶⁴ S. Welack, M. Schreiber, and U. Kleinekathofer, *J. Chem. Phys.* **124**, 044712 (2006).
 - ⁶⁵ S. Welack, U. Kleinekathofer, and M. Schreiber, *J. Lumm.* **119**, 462 (2006).
 - ⁶⁶ U. Kleinekathofer, G. Li, S. Welack, and M. Schreiber, *Europhys. Lett.* **75**, 139 (2006).
 - ⁶⁷ G. Q. Li, M. Schreiber, and U. Kleinekathofer, *Europhys. Lett.* **79**, 27006 (2007).
 - ⁶⁸ F. Grossmann, M. Fischer, T. Kunert, and R. Schmidt, *Chem. Phys.* **322**, 144 (2006).
 - ⁶⁹ J. K. Viljas, F. Pauly, and J. C. Cuevas, *Phys. Rev. B* **77**, 155119 (2008).
 - ⁷⁰ M. Sukharev and M. Galperin, *Phys. Rev. B* **81**, 165307 (2010).
 - ⁷¹ M. Galperin and A. Nitzan, *Phys. Rev. Lett.* **95**, 206802 (2005).
 - ⁷² M. Galperin and A. Nitzan, *J. Chem. Phys.* **124**, 234709 (2006).
 - ⁷³ M. Galperin and S. Tretiak, *J. Chem. Phys.* **128**, 124705 (2008).
 - ⁷⁴ B. D. Fainberg, M. Jouravlev, and A. Nitzan, *Phys. Rev. B* **76**, 245329 (2007).
 - ⁷⁵ B. Fainberg and A. Nitzan, *Phys. Stat. Sol.* **206**, 948 (2009).
 - ⁷⁶ M. Galperin, M. A. Ratner, and A. Nitzan, *Nano Lett.* **9**, 758 (2009).
 - ⁷⁷ M. Galperin, M. A. Ratner, and A. Nitzan, *J. Chem. Phys.* **130**, 144109 (2009).
 - ⁷⁸ T. Seideman, *J. Phys.: Condens. Matter* **15**, R521 (2003).
 - ⁷⁹ N. Lorente, R. Rurali, and H. Tang, *J. Phys.: Condens. Matter* **17**, S1049 (2005).
 - ⁸⁰ R. K. Lake and S. Datta, *Phys. Rev. B* **45**, 6670 (1992).
 - ⁸¹ R. K. Lake and S. Datta, *Phys. Rev. B* **46**, 4757 (1992).
 - ⁸² D. Segal and A. Nitzan, *J. Chem. Phys.* **117**, 3915 (2002).
 - ⁸³ M. J. Montgomery, T. N. Todorov, and A. P. Sutton, *J. Phys.: Condens. Matter* **14**, 5377 (2002).
 - ⁸⁴ B. N. J. Persson and P. Avouris, *Surf. Sci.* **390**, 45 (1997).
 - ⁸⁵ A. P. Horsfield, D. R. Bowler, H. Ness, C. G. Sanchez, T. N. Todorov, and A. J. Fisher, *Rep. Prog. Phys.* **69**, 1195 (2006), and references therein.
 - ⁸⁶ M. Galperin, A. Nitzan, and M. A. Ratner, *Phys. Rev. B* **75**, 155312 (2007).
 - ⁸⁷ M. Galperin, M. A. Ratner, and A. Nitzan, *J. Phys.: Condens. Matter* **19**, 103201 (2007), and references therein.
 - ⁸⁸ J. T. Lu and J.-S. Wang, *Phys. Rev. B* **76**, 165418 (2007).
 - ⁸⁹ Q.-f. Sun and X. C. Xie, *Phys. Rev. B* **75**, 155306 (2007).
 - ⁹⁰ Y. C. Chen, *Phys. Rev. B* **78**, 233310 (2008).
 - ⁹¹ R. D'Agosta and M. Di Ventra, *J. Phys.: Condens. Matter* **20**, 374102 (2008).
 - ⁹² A. Pecchia, G. Romano, and A. Di Carlo, *Phys. Rev. B* **75**, 035401 (2007).
 - ⁹³ G. Schulze, et al., *Phys. Rev. Lett.* **100**, 136801 (2008).
 - ⁹⁴ S. V. Rotkin, V. Perebeinos, A. G. Petrov, and P. Avouris, *Nano Lett.* **9**, 1850 (2009).
 - ⁹⁵ B. H. Wu and J. C. Cao, *J. Phys.: Condens. Matter* **21**, 8 (2009).
 - ⁹⁶ Q. A. Chen and Y. M. Zhang, *Commun. Theor. Phys.* **54**, 171 (2010).
 - ⁹⁷ E. Pop, *Nano Res.* **3**, 147 (2010), and references therein.
 - ⁹⁸ C. A. Santini and et al., *Nanotechnology* **22**, 395202 (2011).
 - ⁹⁹ N. Agrait, C. Untiedt, G. Rubio-Bollinger, and S. Vieira, *Phys. Rev. Lett.* **88**, 216803 (2002).
 - ¹⁰⁰ Z. F. Huang, B. Q. Xu, Y. C. Chen, M. Di Ventra, and N. J. Tao, *Nano Lett.* **6**, 1240 (2006).
 - ¹⁰¹ Z. Huang, F. Chen, R. D'Agosta, P. A. Bennett, M. Di Ventra, and N. Tao, *Nature Nanotech.* **2**, 698 (2007).
 - ¹⁰² M. Tsutsui, M. Taniguchi, and T. Kawai, *Nano Lett.* **8**, 3293 (2008).
 - ¹⁰³ M. Tsutsui, M. Taniguchi, K. Yokota, and T. Kawai, *Appl. Phys. Lett.* **96**, 103110 (2010).
 - ¹⁰⁴ M. Freitag, M. Steiner, Y. Martin, V. Perebeinos, Z. Chen, J. C. Tsang, and P. Avouris, *Nano Lett.* **9**, 1883 (2009).
 - ¹⁰⁵ M. Steiner, M. Freitag, V. Perebeinos, J. C. Tsang, J. P. Small, M. Kinoshita, D. N. Yuan, J. Liu, and P. Avouris, *Nature Nanotech.* **4**, 320 (2009).
 - ¹⁰⁶ The fact the molecule induced effect dominates can be seen by comparing Figures 4a and 4d of Ref. 12, which show that the effective temperature of the electronic Raman continuum in a molecular junction that carries a current of ~ 2 mA exceeds that of a bare junction with ten times larger current.
 - ¹⁰⁷ M. Moskovits, *Rev. Mod. Phys.* **57**, 783 (1985).
 - ¹⁰⁸ E. Burstein, Y. J. Chen, C. Y. Chen, S. Lundquist, and E. Tosatti, *Solid State Commun.* **29**, 567 (1979).
 - ¹⁰⁹ J. I. Gersten, R. L. Birke, and J. R. Lombardi, *Phys. Rev. Lett.* **43**, 147 (1979).
 - ¹¹⁰ W. Akemann and A. Otto, *Surf. Sci.* **307**, 1071 (1994).
 - ¹¹¹ T. Itoh, V. Biju, M. Ishikawa, Y. Kikkawa, K. Hashimoto, A. Ikehata, and Y. Ozaki, *J. Chem. Phys.* **124**, 134708 (2006).
 - ¹¹² O. P. Varnavski, M. B. Mohamed, M. A. El-Sayed, and T. Goodson, *J. Phys. Chem. B* **107**, 3101 (2003).
 - ¹¹³ E. Dulkeith, T. Niedereichholz, T. A. Klar, J. Feldmann, G. von Plessen, D. I. Gittins, K. S. Mayya, and F. Caruso, *Phys. Rev. B* **70**, 205424 (2004).
 - ¹¹⁴ Considerations of coupling magnitudes imply that energy transfer from individual electron-hole pair excitations is an unlikely event. This does not preclude the notion that

radiative emission from those electron-hole pairs that couple to the plasmon (those generated by radiationless decay of the plasmon) is enhanced relative to other e-h pairs. The bottom line agrees with the observations of Refs. 112,113: emission is enhanced at the plasmon frequency range.

¹¹⁵ B. Pettinger, J. Chem. Phys. **85**, 7442 (1986).

¹¹⁶ J. R. Lombardi and R. L. Birke, J. Phys. Chem. C **114**,

7812 (2010).

¹¹⁷ M. Galperin and A. Nitzan, J. Phys. Chem. Lett. **2**, 2110 (2011).

¹¹⁸ M. Galperin, A. Nitzan, and M. A. Ratner, Phys. Rev. Lett. **96**, 166803 (2006).

¹¹⁹ G. D. Mahan, *Many-particle physics* (Plenum press, New York, 2000).